

# Mechanism of adhesion between protein-based hydrogels and plasma treated polypropylene backing

Rony Snyders<sup>a</sup>, Oleg Zabeida<sup>a</sup>, Christophe Roberges<sup>b</sup>, Kirill I. Shingel<sup>b</sup>, Marie-Pierre Faure<sup>b</sup>, Ludvik Martinu<sup>a</sup>, Jolanta E. Klemberg-Sapieha<sup>a,\*</sup>

<sup>a</sup> Department of Engineering Physics, Ecole Polytechnique, Box 6079, Station "Centre ville", Montreal, Que., Canada H3C 3A7

<sup>b</sup> Biortificial Gel Technologies Inc., 400, De Maisonneuve Ouest, Suite 1156, Montreal, Que., Canada H3A 1L4

Received 4 July 2006; accepted for publication 6 September 2006

Available online 27 September 2006

## Abstract

We studied the mechanism of adhesion between N<sub>2</sub> plasma treated polypropylene (PP/N<sub>2</sub>) backing and a hybrid hydrogel (HG) produced by chemical crosslinking between poly(ethylene glycol) and soy albumin. The work of adhesion, measured by peel testing, was found to be 25 times higher for PP/N<sub>2</sub> compared to untreated PP ( $\approx 5.0$  J/m<sup>2</sup> versus  $\approx 0.2$  J/m<sup>2</sup>). In order to understand the adhesion mechanism, we performed a detailed analysis of the surface chemical composition of PP and PP/N<sub>2</sub> using X-ray photoelectron spectroscopy (XPS), chemical derivatization and attenuated total reflectance infra-red (ATR-IR) measurements. The results confirm incorporation of different nitrogen- (amine, amide, . . .) and oxygen- (hydroxyl, carboxyl, . . .) containing chemical groups on the PP/N<sub>2</sub> surface. The derivatized functions were primary amine, hydroxyl, carboxyl and carbonyl groups. Chemical derivatization reactions validated the XPS results (except for carbonyl groups), and they clearly underlined the essential role of primary amine groups in the adhesion process. In fact, after derivatization of the amine functions, the work of adhesion was found to be  $0.41 \pm 0.12$  J/m<sup>2</sup>. Participation of amine groups in the formation of covalent bonds at the interface between PP/N<sub>2</sub> and HG was directly confirmed by ATR-IR measurements.

© 2006 Elsevier B.V. All rights reserved.

**Keywords:** Hydrogels; Polypropylene; Plasma treatment; Adhesion; XPS; Chemical derivatization; ATR-IR

## 1. Introduction

Hydrogel (HG) is a water-swollen polymer network of either natural or synthetic origins having a great affinity for water [1]. Strong interests in the development of novel synthetic HG can be attributed to their unique combination of properties such as biocompatibility, permeability, hydrophilicity and others. Recently, hybrid HGs based on blends of synthetic and natural polymers have been successfully developed [2]. They are often referred to as "bioartificial polymeric materials" [3].

HGs are used in wound dressing, cosmetic patches or in drug delivery devices. The main limitation of HGs with

high content of water (up to 96%) is, however, their fragility [4]. Therefore, in order to facilitate their handling and manipulation, they require backing, usually made out of a polymer film.

In general, adhesion between HGs and polymer backing is very poor. In order to improve the adhesive properties of polymers, various techniques are available for surface modification such as wet chemical, flame and corona treatments [5]. Among the various methods, cold plasma treatment is a well-established method for improving adhesive properties of polymeric substrates [6–10].

It is accepted that, depending on the gas composition and plasma conditions, ions, fast neutrals, radicals and vacuum ultra-violet (VUV) radiations participate in the treatment of polymer surface, resulting in etching, chemical functionalization, cleaning, activation, cross-linking and

\* Corresponding author. Tel.: +1 514 340 5747; fax: +1 514 340 3218.  
E-mail address: [jsapieha@polymtl.ca](mailto:jsapieha@polymtl.ca) (J.E. Klemberg-Sapieha).

formation of an interfacial region (interphase), that all in synergy, contribute to adhesion [6–14].

In numerous instances, plasma treatment in oxygen has proven very useful due to surface cleaning, surface activation and microroughening, as demonstrated for metal films (Cr, Cu) on poly-imide [15] or self adhesion in polyethylene–polyethylene and polyethylene–polyethylene terephthalate laminates [13], while surface roughening by Ar<sup>+</sup> ions led to improved adhesion of Cu on poly-tetra-fluoroethylene [16].

Frequently, plasma treated polymer surfaces undergo ageing effects due to reactions with the surrounding atmosphere, but importantly, due to thermodynamically driven reorientation of the introduced surface chemical groups into the polymer bulk [9,11,17]. In this respect, such hydrophobic recovery can be inhibited by energetic photon-induced (vacuum ultraviolet radiation, VUV) crosslinking [9–11,18,19].

Many studies pointed out the beneficial role of surface treatment in nitrogen plasma giving rise to strong covalent bonds at the film-surface interface containing nitrogen chemical linkages [20]. For example, this has been demonstrated for improving adhesion of metals on polyolefins [21] and on fluoropolymers [22], as well as inorganic optical coatings on polycarbonate [14] and poly-methyl-methacrylate [18].

Most of the papers related to adhesion improvement by plasma treatment are unanimous in attributing an important role to the chemical functionalization of the polymer surface by polar chemical groups [5–11,13,21–24]. They significantly improve adhesion between the treated polymer and the other component by interactions ranging from the rather weak Van der Waals or acid/base interactions to the strong covalent bonding. In this work, we focused our attention to the chemical functionalization effect, aiming at determining the role of the most important chemical functions grafted during the plasma treatment and leading to highest adhesion of HG to polypropylene (PP). In fact, we have previously shown, that surface treatment of PP in low pressure N<sub>2</sub> plasma (PP/N<sub>2</sub>) leads to, at least, a 25-fold increase of the work of adhesion ( $W_A$ ) when optimum conditions are used [25].

The study of the chemical groups introduced to the polymer surface by N<sub>2</sub> plasma is rather complex because of the broad range of incorporated species [12,23]. In addition, the binding energy shift of the C1s spectra measured by X-ray Photoelectron Spectroscopy (XPS) for the chemical functions, such as amine, hydroxyl, carbonyl, amide, and carboxyl is often too small to allow an accurate spectral curve fitting [26]. Therefore, only a combination of several complementary analytical techniques such as chemical derivatization reactions, XPS [24,27,28] and attenuated total reflectance infra-red (ATR-IR) provide appropriate information about the interface chemistry.

Specifically, chemical derivatization was developed to selectively label surface functional groups of interest, suitable for further analysis by XPS [26–29] and mass spec-

trometry [28–33]. The principle of the technique is to selectively graft to specific chemical groups a molecule containing a chemical element (F, Cl, I, ...) that is easily detectable by the analysis method.

The objectives of the present work were is to perform a complete chemical analysis of PP/N<sub>2</sub> using chemical derivatization, XPS and ATR-IR measurements in order to assess the adhesion mechanism between PP/N<sub>2</sub> and HG. Indeed, by selectively blocking specific chemical functions present on the PP/N<sub>2</sub> surface and by measuring the work of adhesion ( $W_A$ ) for every derivatized sample, we were able to determine the chemical groups responsible for the adhesion improvement.

## 2. Experimental setup

### 2.1. Synthesis of the hydrogels

The PEG-based HG used in this study was prepared at Bioartificial Gel Technology, Montreal, Canada. The HG was obtained by chemical crosslinking of bi-functionalized (using 4-nitrophenylchloroformate) poly(ethylene glycol) (PEG) and soy albumin protein. During this reaction a para-nitrophenol molecule is liberated and PEG forms a urethane linkage with the free amino-groups of the soy protein. As a result, stable urethane linkages between a bi-polymer and PEG are formed. Hydrogels are then washed in a phosphate buffer solution (PBS) at a pH of 7.2–7.4 to remove unreacted components. More details have been published previously [2,34,35]. For this study, water swollen HG samples were synthesized from 1:1 aqueous solutions of soy protein with a 12 wt.% of soy albumin and 22 wt.% of PEG.

### 2.2. Plasma treatment of polypropylene

N<sub>2</sub> plasma treatments were performed in a radio-frequency (RF, 13.56 MHz) plasma system (Fig. 1) equipped with a roll-to-roll mechanism. The system consisted of a turbomolecularly pumped aluminium vessel with a 12 × 12 cm RF electrode (made of copper). Twelve centimeter wide polypropylene (PP) films, in contact with the RF-powered electrode, were moved through the plasma zone at a speed of about 30 cm/min. The RF power was adjusted at 100 W leading to a self-bias voltage of –300 V on the electrode, while the N<sub>2</sub> flow rate was fixed to 220 sccm and the pressure to 200 mTorr. All PP samples were treated with a residence time in the plasma of 25 s, corresponding to the optimum treatment duration determined previously [25].

### 2.3. Adhesion measurement

The work of adhesion,  $W_A$ , was measured using a slip-peel test instrument (Peel Tester Instrumentors SP-103B-3M45) with a load cell of 0–19 g at a peel-off rate of 2.2 cm/min. The measuring specimen consisted of two

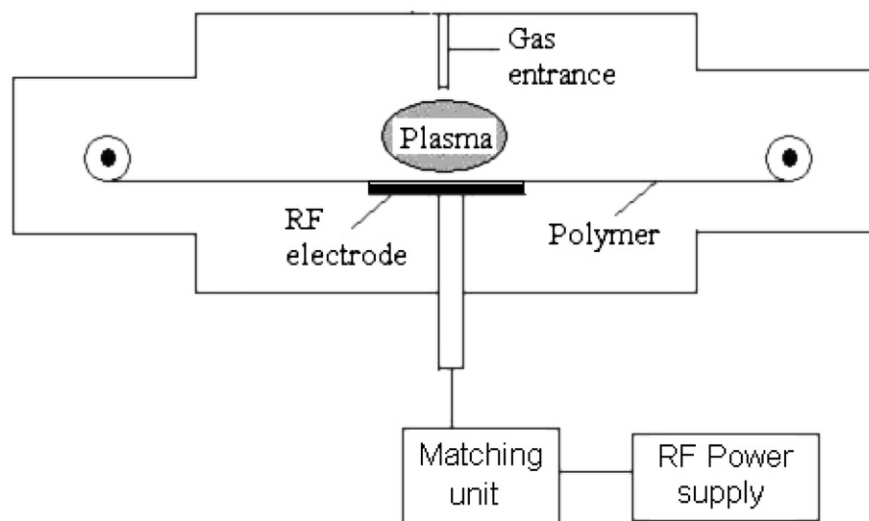


Fig. 1. Schematic of the RF N<sub>2</sub> plasma treatment chamber.

pieces of  $6 \times 6 \text{ cm}^2$  PP/N<sub>2</sub> attached to both sides of  $3 \times 3 \text{ cm}^2$  HG samples. After attachment, 15 min waiting time was allowed for interaction between PP/N<sub>2</sub> and the HG.

For peel force measurement, one piece of PP/N<sub>2</sub> attached to the HG was fixed to the moving element of the slip-peel tester using an adhesive tape, and the other piece was attached to the load gauge at a  $90^\circ$  angle using a clamp (Fig. 2a). In this experiment, the force ( $F$ ) necessary to peel-off the PP/N<sub>2</sub> specimen from the HG was recorded as a function of time ( $t$ ) (Fig. 2b). The area under the  $F = f(t)$  curve corresponding to the necessary  $W_A$  to peel off the PP/N<sub>2</sub> from the HG was determined as:

$$W_A = \frac{v}{S} \int_0^{l/v} F(t) dt, \quad (1)$$

where  $v$  is the displacement speed,  $l$  is the sample length along the displacement direction,  $S$  is the sample surface, and  $t$  is the duration of the measurement.

#### 2.4. XPS characterization

XPS analyses were performed in a VG-ESCALAB 3 Mark II system pumped to a base pressure around  $3 \times 10^{-10}$  Torr. The XPS data were collected using a non-monochromated Mg K <sub>$\alpha$</sub>  radiation at 1253.6 eV with a 0.8 eV resolution. Photoelectrons were collected at a take-off angle of  $\theta = 0^\circ$  from surface normal.

For all samples, survey spectra were recorded with a 50 eV pass energy, while the high resolution spectra in the regions of interest (O1s, C1s, N1s, Cl2p and F1s peaks) were obtained with a 20 eV pass energy. Atomic concentrations were derived from the peak areas by using photoionization cross sections calculated by Wagner et al. [36].

Shirley-type background subtraction was used prior to peak separation of non-smoothed XPS spectra. The full width at half maximum (FWHM) of the different carbon

peaks was fixed at 1.65 eV, and the shape ratio (Gaussian to Lorentzian) was 60%. Chemical shifts of the different carbon-containing groups which compose the C1s peak were based on the values proposed by different authors in the literature: they are reported in Table 1 with the corresponding chemical group. The chemical shift of the carbon peak is referred to aliphatic carbon at 285.0 eV. The curve fitting quality was evaluated by the Chi-square convergence.

#### 2.5. Chemical derivatization

Chemical derivatizations of PP/N<sub>2</sub> were carried out in vapour phase with para-chlorobenzaldehyde (pCB, Alfa Aesar, 95% of purity) for primary amine (C–NH<sub>2</sub>), trifluoroacetic anhydride (tFAA, Alfa Aesar, 95% of purity) for hydroxyl (C–OH), and 2,2,2-trifluoroethanol (tFE, Alfa Aesar, 95% of purity) for carboxyl (O–C=O) groups. It is important to emphasize that tFAA also reacts with primary and secondary amine functionalities.

Derivatization reactions with pCB vapours were performed in an oven at 55 °C for time periods varying from 30 min to 96 h as proposed by Chevallier et al. [27]. Derivatization with tFAA and tFE vapours were carried out in vials at room temperature. According to the method described by Markkula et al. [31], the reagents were introduced to the vial with the PP/N<sub>2</sub> sample, and the derivatization time was 24 h.

Liquid phase derivatization of carbonyl (C=O) was performed with a saturated solution (10 mg/ml) of 2,5-difluorophenylhydrazine (dFPH, Alfa Aesar, 97% purity) in dehydrated ethanol. The samples were placed in the solution for 20 min and then washed thoroughly with anhydride ethanol [31].

After each chemical derivatization reaction, the derivatized samples were outgassed at room temperature in vacuum ( $\sim 10^{-6}$  Torr) during 1 h, followed by XPS analysis and adhesion measurements.

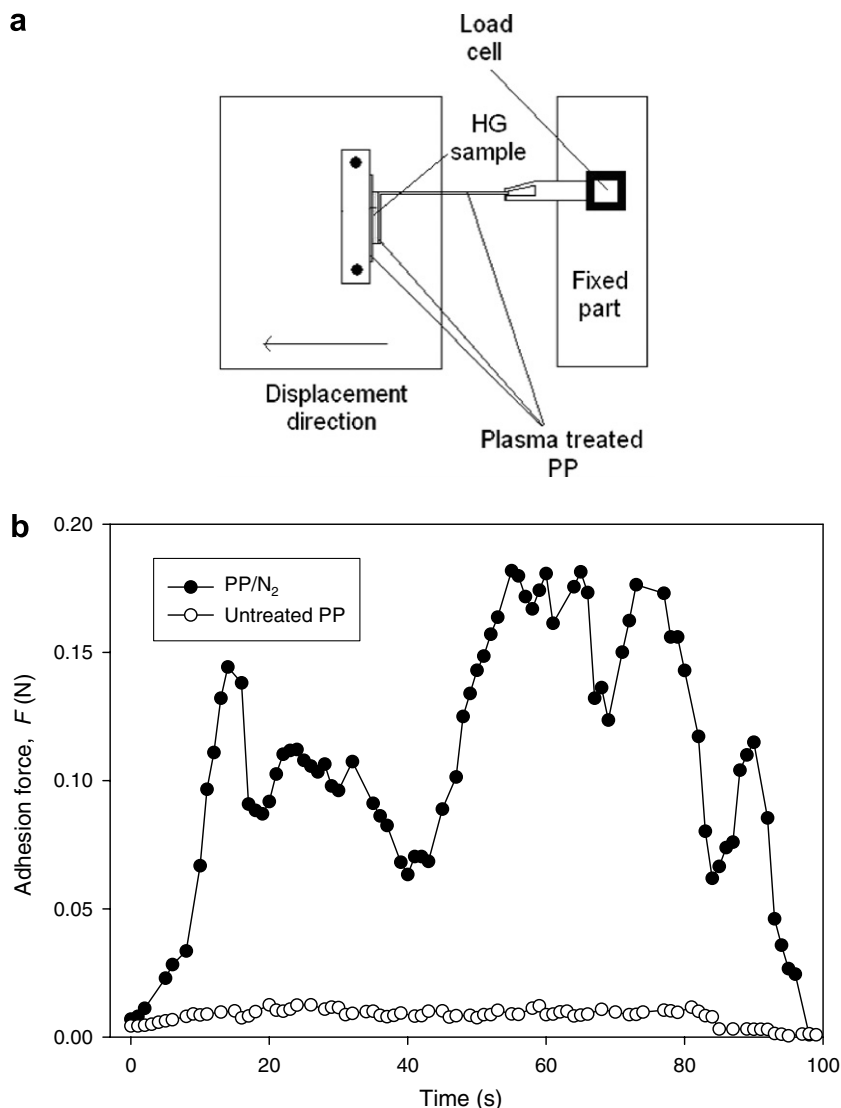


Fig. 2. Schematic of the adhesion measurement system (a) and a typical measured adhesion curve (b).

Table 1

Chemical shift corresponding to different types of carbon linkages observed after deconvolution of the C1s peak

| Assignment       | Chemical shift (eV) | Carbon label   | References |
|------------------|---------------------|----------------|------------|
| C–C and C–H      | 285.0               | C <sub>1</sub> | [12,13]    |
| C–N              | 285.7               | C <sub>2</sub> | [12]       |
| C–Cl and/or C–O  | 286.7               | C <sub>3</sub> | [12,38]    |
| C=NH             | 286.9               | C <sub>4</sub> | [12]       |
| C=O and/or N–C=O | 288.3               | C <sub>5</sub> | [12,13]    |
| O–C=O            | 289.2               | C <sub>6</sub> | [12]       |
| CF <sub>3</sub>  | 293.0               | C <sub>7</sub> | [28]       |

In order to verify the effect of the derivatization process on the virgin PP, for example solubility of the agent used for derivatization inside the polymer, in every case, a pure PP reference sample has been submitted to the same reaction. Moreover, as mentioned above, during derivatization of primary amine, it is necessary to heat the PP/N<sub>2</sub> specimens to 55 °C. This may possibly lead to accelerated ageing

of the polymer surface. To verify changes in the chemical composition of PP/N<sub>2</sub> due to the heat treatment, PP/N<sub>2</sub> samples were annealed for 24 h at 55 °C (PP/N<sub>2</sub>/annealed), followed by XPS analysis.

## 2.6. ATR-IR characterization

Interaction between soy proteins and PP/N<sub>2</sub> (PP/N<sub>2</sub>-Prot) has been studied by ATR-IR. A piece of PP/N<sub>2</sub> was in contact for 15 min with saturated 96 vol.% aqueous solution of soy albumin from Archer Daniels Midland Co. Then, the sample was thoroughly washed with water and dried at room temperature during 8 h. PP/N<sub>2</sub>-Prot and PP/N<sub>2</sub> samples were analyzed by ATR-IR spectroscopy at 45° incidence using a trapezoidal Ge crystal (50 × 20 × 2 mm) with 45° facet angle (Single Pass Trapezoid Plate, Harrick Scientific Corp.) in a Digilab FTS-3000 Excalibur Seri spectrometer equipped with a deuterated triglycine sulphate detector. The background was

determined with a Ge prism and subtracted from the measured spectra.

### 3. Results and discussion

#### 3.1. XPS study of PP and PP/N<sub>2</sub> surfaces

In the first part of this study, we performed a detailed analysis of the plasma treated PP surfaces. Fig. 3 presents high resolution C1s spectra and relevant curve fitting for PP, PP/N<sub>2</sub> and the derivatized PP/N<sub>2</sub> samples. Tables 2 and 3 report a summary of the chemical composition and of the curve fitting data.

The results show that untreated PP already contains 5.4 at.% of O, while the curve fitting reveals that O is not bonded to C. Indeed, the C1s peak of PP is entirely composed of the aliphatic component (C<sub>1</sub> at 285.0 eV). We therefore assume that oxygen is adsorbed on the PP surface or dissolved in the polymer as an impurity.

Exposure of PP to N<sub>2</sub> plasma leads to a substantial restructuring of the chemical composition of PP, namely incorporation of nitrogen- and oxygen-containing groups: broad scan analysis reveals 13.2 at.% of N and 14.9 at.% of O for PP/N<sub>2</sub> (Table 2).

The high content of O on PP/N<sub>2</sub> has two origins: (i) incorporation of O during the plasma treatment from the residual gases present in the treatment chamber (water vapor and oxygen), and (ii) reaction with oxygen or water vapor after exposure to the atmosphere. Indeed, it is well known that after plasma treatment of polymers, unreacted radicals present at the surface readily react with the atmospheric gaseous species. Similar observations were made by Frances et al. for polystyrene and PP surfaces treated in Ar plasma [38], confirming post-treatment incorporation of O at the polymer surface.

The C1s peak for PP/N<sub>2</sub> (Fig. 3) shows an intense broadening towards high binding energy, giving evidence of O and N incorporation. From curve fitting results (Table 3) we expect the presence of C–N (C<sub>2</sub>), C–O (C<sub>3</sub>), C=O and/or N–C=O (C<sub>5</sub>), and O–C=O (C<sub>6</sub>) bonds at the surface. The most abundant nitrogen-containing function introduced at the PP/N<sub>2</sub> surface is amine (C–N). Since the XPS resolution of the spectrometer used in this study is only 0.8 eV, it is impossible to distinguish primary, secondary and tertiary amines. From the curve fitting results, the C<sub>2</sub> peak at 285.7 eV assigned to C–N represents 22.1% of C present in this form at the surface (Table 3). The C<sub>3</sub>, C<sub>5</sub> and C<sub>6</sub> peaks, assigned to C–O, C=O and/or N–C=O and O–C=O groups, respectively, represent 8.8%, 6.3% and 0.1% of the carbon.

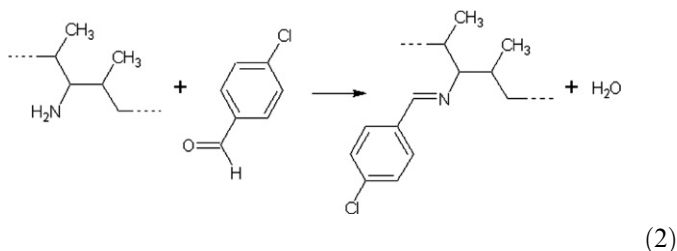
#### 3.2. Chemical derivatization

In order to validate the assignments of the components of the C1s peak, we performed chemical derivatizations of the expected chemical functions introduced at the PP/N<sub>2</sub>

surface. The studied functionalities were primary amine (C–NH<sub>2</sub>), hydroxyl (C–OH), carboxyl (HO–C=O) and carbonyl groups (C=O).

##### 3.2.1. Chemical derivatization of primary amine

Eq. (2) describes the condensation reaction occurring during the derivatization of primary amine using pCB. This reaction is known to be very selective for C–NH<sub>2</sub>, as recently shown by Chevallier et al. [27] using different surfaces presenting only one functionality: oxydianiline (amino groups), polyacrilamide (amide groups), and poly(acrylic acid) (carboxyl groups), polyacrylonitrile (nitrile groups). We conclude from Eq. (2), that for every C–NH<sub>2</sub> which reacts with pCB, we introduce two elements which are not present at the virgin surface, namely (i) Cl atom (C–Cl, C<sub>3</sub>, 286.7 eV), and (ii) C=N groups (C<sub>4</sub>, 287.0 eV).



Tables 2 and 3 show, respectively, the composition and percentage of different chemical groups determined by XPS for PP, PP/N<sub>2</sub> and the derivatized PP and PP/N<sub>2</sub> surfaces. We observe incorporation of Cl (2 at.%) after derivatization of PP/N<sub>2</sub>, while no Cl was detected on pure PP surface. The C1s peak following derivatization was restructured (Fig. 3 and Table 3). We observe a decrease of peak C<sub>2</sub> from 22.1% to 17.5%, and an increase of peak C<sub>3</sub> from 8.8% to 10.3%.

The decrease of C<sub>2</sub> is attributed to the consumption of C–NH<sub>2</sub>, and the increase of C<sub>3</sub> (C–OH) is attributed to the appearance of C–Cl bonds which exhibit a chemical shift similar to C–OH bonds [37,39]. These results suggest the consumption of C–NH<sub>2</sub> groups and subsequent incorporation of Cl and C=N on the PP/N<sub>2</sub> surface by the derivatization reaction with pCB, clearly confirming the presence of C–NH<sub>2</sub>.

Annealing of PP/N<sub>2</sub> (PP/N<sub>2</sub>/annealed), was found to increase the O concentration (from 14.9 at.% to 15.6 at.%), while no significant changes in N were observed (see Table 2). We can therefore conclude that heating does not lead to artifacts during C–NH<sub>2</sub> derivatization.

We studied in detail the C–NH<sub>2</sub> derivatization kinetics by evaluating the surface chemical composition as a function of derivatization time (Fig. 4a). We found that the surface composition stabilizes after 1.5 h of derivatization when the Cl concentration reaches its highest value of 2 at.%. This value is slightly higher than the one determined by Chevallier et al. [27]. Therefore, the derivatization duration of 24 h for the pCB reaction was considered appropriate.

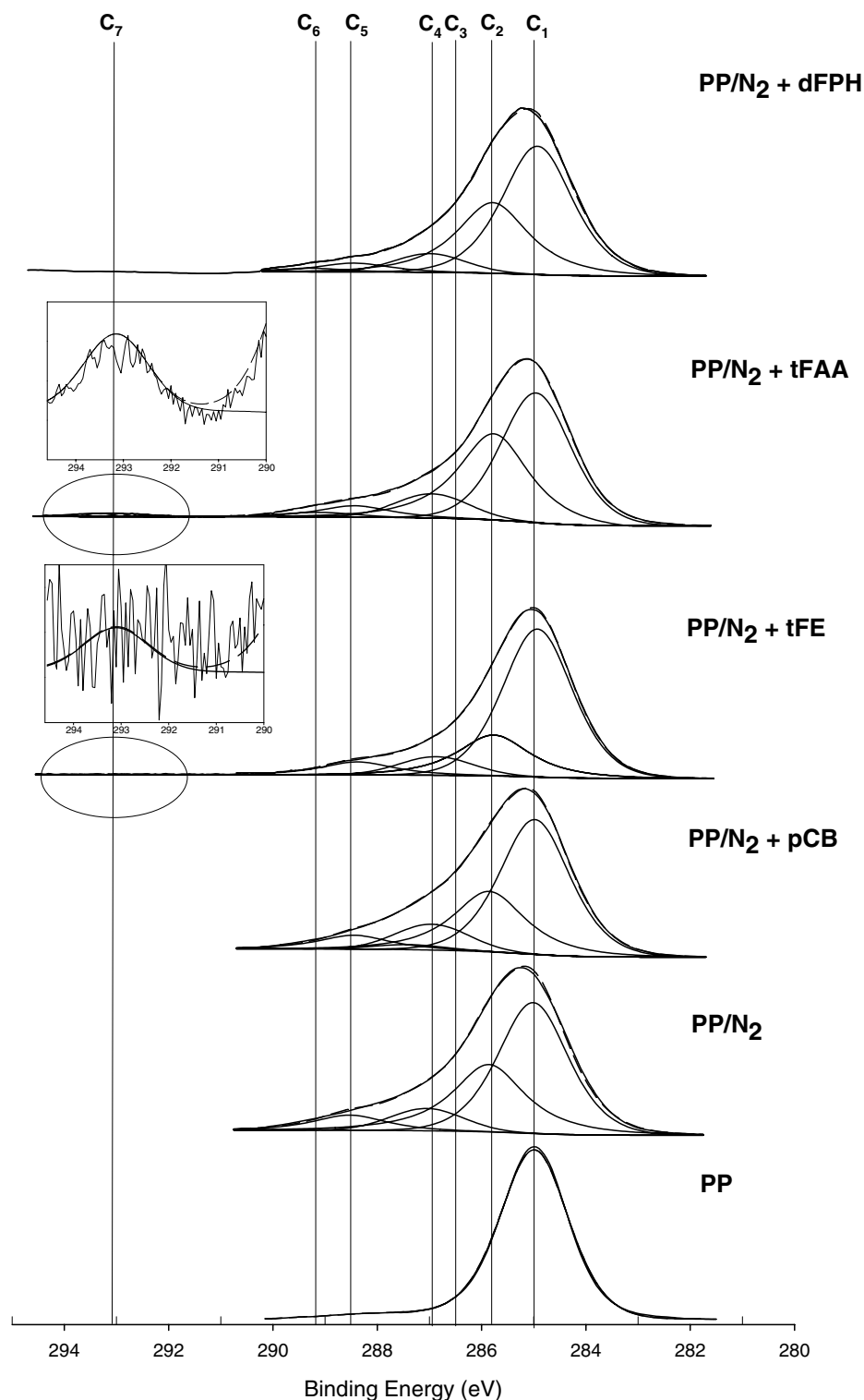


Fig. 3. Evolution of the C<sub>1s</sub> peak measured by XPS following chemical derivatization.

The value of 2 at.% of C<sub>1</sub> after 24 h of derivatization appears rather low compared to the concentration of amine groups determined from high resolution XPS spectra (Fig. 3 and Table 3). This can be explained by the following arguments: (i) the derivatization reaction of amine groups which used an aldehyde is efficient only for primary amines

(C–NH<sub>2</sub>) [40,41]; therefore, secondary and tertiary amines which also contribute to the C<sub>2</sub> peak are not derivatized, and (ii) a certain part of C–NH<sub>2</sub> introduced by N<sub>2</sub> plasma treatment is not available for derivatization due to the thermally induced polymer chains rotation which hides the active chemical groups inside the polymer [42].

Table 2  
Chemical composition determined by XPS

| Samples                     | C (at.%) | O (at.%) | N (at.%) | Cl (at.%) | F (at.%) |                                  |
|-----------------------------|----------|----------|----------|-----------|----------|----------------------------------|
| PP                          | 94.6     | 5.4      | –        | –         | –        |                                  |
| PP/N <sub>2</sub>           | 71.9     | 14.9     | 13.2     | –         | –        |                                  |
| PP/N <sub>2</sub> /annealed | 70.4     | 15.6     | 13.0     | –         | –        |                                  |
| PP/N <sub>2</sub> + pCB     | 73.6     | 15.8     | 8.6      | 2.0       | –        | Primary amine derivatization     |
| PP + pCB                    | 95.9     | 4.1      | –        | –         | –        |                                  |
| PP/N <sub>2</sub> + tFE     | 72.0     | 13.5     | 13.0     | –         | 1.5      | Carboxyl derivatization          |
| PP + tFE                    | 95.8     | 4.2      | –        | –         | –        |                                  |
| PP/N <sub>2</sub> + tFAA    | 68.6     | 9.8      | 12.1     | –         | 5.5      | Hydroxyl (+amine) derivatization |
| PP + tFAA                   | 93.0     | 6.0      | –        | –         | 0.9      |                                  |
| PP/N <sub>2</sub> + dFPH    | 76.4     | 9.8      | 13.9     | –         | –        | Carbonyl derivatization          |
| PP + dFPH                   | 94.8     | 5.2      | –        | –         | –        |                                  |

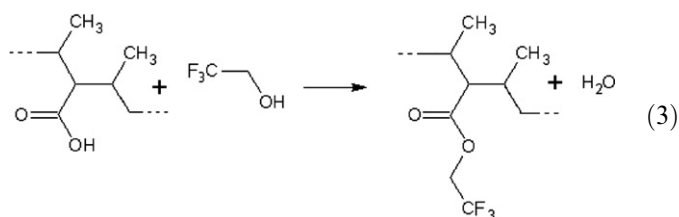
Table 3  
Percentage of different carbon-containing groups

| Sample                   | C <sub>1</sub> | C <sub>2</sub> | C <sub>3</sub> | C <sub>4</sub> | C <sub>5</sub> | C <sub>6</sub> | C <sub>7</sub> |
|--------------------------|----------------|----------------|----------------|----------------|----------------|----------------|----------------|
| PP                       | 100.0          | –              | –              | –              | –              | –              | –              |
| PP/N <sub>2</sub>        | 62.7           | 22.1           | 8.8            | –              | 6.3            | 0.1            | –              |
| PP/N <sub>2</sub> + pCB  | 64.0           | 17.5           | 10.3           | 2.0            | 6.1            | 0.1            | –              |
| PP/N <sub>2</sub> + tFE  | 68.8           | 17.3           | 7.1            | –              | 6.4            | 0.2            | 0.2            |
| PP/N <sub>2</sub> + tFAA | 60.4           | 22.4           | 7.9            | –              | 6.0            | 1.9            | 1.4            |
| PP/N <sub>2</sub> + dFPH | 63.0           | 23.2           | 8.5            | –              | 5.1            | 0.2            | 0.0            |

### 3.2.2. Chemical derivatization of carboxyl, hydroxyl and carbonyl groups

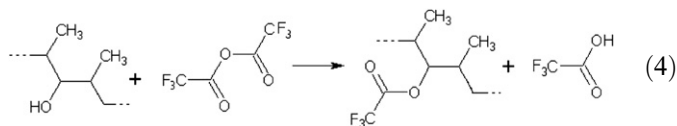
Chemical derivatization reactions of further chemical groups on the PP/N<sub>2</sub> surface are described by Eqs. (3)–(5), respectively, for HO–C=O, C–OH and C=O. Chemical composition of the different derivatized samples are reported in Table 2 in comparison with PP derivatized under the same conditions. XPS spectra of the C1s peak and their curve fitting are presented in Fig. 3 and their analysis is presented in the subsequent section.

**3.2.2.1. Derivatization of carboxyl groups.** Chemical derivatization of PP/N<sub>2</sub> by tFE introduces 1.5 at.% of F on the surface. In Fig. 3 and Table 3, we observe the presence of C<sub>7</sub> due to CF<sub>3</sub> bonds which confirms the presence of the carboxyl (HO–C=O) groups at the PP/N<sub>2</sub> surface.



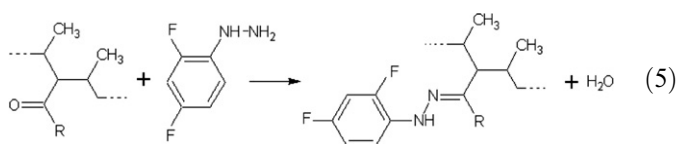
**3.2.2.2. Derivatization of hydroxyl groups.** As already pointed out in Section 2, tFAA reacts not only with the C–OH groups but also with primary and secondary amines to form amide groups [43]. Therefore, any approach to quantification has to be made with caution. We observed

that the derivatization of PP/N<sub>2</sub> by tFAA leads to the introduction of 9.5 at.% of F at the surface (Table 2). Curve fitted spectra (Fig. 3 and Table 3) show the presence of C<sub>7</sub> (1.4%) corresponding to the CF<sub>3</sub> (293.0 eV) peak and, in comparison with PP/N<sub>2</sub>, the C<sub>6</sub> peak intensity increases from 0.1% to 1.9% due to the presence of O–C=O (289.2 eV). The latter one appears at the surface after formation of an ester bond between tFAA and C–OH. One can note that contribution of C<sub>5</sub> (288.3 eV), corresponding (at least partially) to N–C=O bonds, does not appreciably change after tFAA derivatization. This observation indicates that hydroxyl groups are, in our case, more efficiently derivatized than amine groups, since the reaction between amine and anhydride produces amide functionalities.



For comparison, the same treatment by tFAA has been performed on untreated PP. We observe 0.9 at.% of F (Table 2) assumed to be related to traces of –OH groups (impurities) present at the PP surface.

**3.2.2.3. Derivatization of carbonyl groups.** Since the peaks due to C=O and N–C=O are completely overlapped (C<sub>5</sub>, Table 1), their contribution can only be distinguished by chemical derivatization. During the derivatization of the C=O groups with dFPH, one expects the presence of C–F and C=N bonds (Eq. (5)). However, no F was detected (Table 2) and no restructuring of the C1s peak was observed; this suggests the absence of C=O groups at the PP/N<sub>2</sub> surface. Therefore, we conclude that C<sub>5</sub> is mainly related to N–C=O functions.



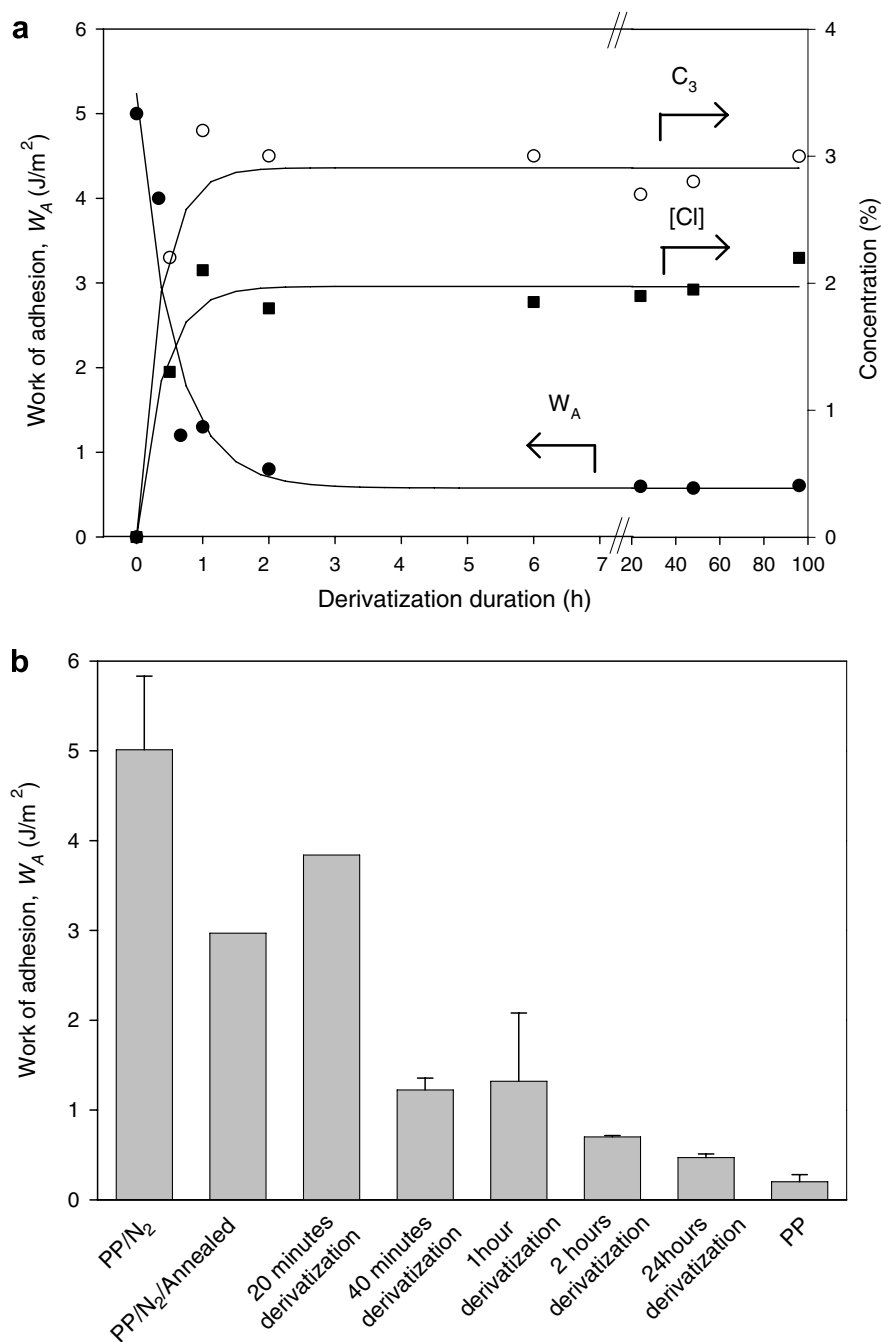


Fig. 4. Correlation between  $W_A$  and the surface composition, namely Cl at.% and C=N bond contribution to the Cls peak (a) and the duration of the amine groups derivatization (b).

### 3.3. Study of adhesion between PP/N<sub>2</sub> and HG

#### 3.3.1. Adhesion evaluation

In order to study the importance of each chemical function introduced by the N<sub>2</sub> plasma treatment of PP on the adhesion of HG, we measured  $W_A$  for PP/N<sub>2</sub> samples derivatized for specific functional groups. Derivatization, described in the previous section, leads to selective blocking of different chemical groups introduced during the plasma treatment. These groups cannot participate anymore in the adhesion process between PP/N<sub>2</sub> and HG. In the following,

we assume a weak influence of the newly introduced elements and groups (–CF<sub>3</sub>, –Cl) at the derivatized PP/N<sub>2</sub> surface on the adhesion.

$W_A$  values for untreated PP, PP/N<sub>2</sub>, PP/N<sub>2</sub>/annealed, PP/N<sub>2</sub>/24 h and for PP/N<sub>2</sub>/derivatized for different functional groups are summarized in Table 4.  $W_A$  increases 25 times immediately after N<sub>2</sub> plasma treatment of PP; however, after 24 h, with or without annealing,  $W_A$  decreases by about 40% of its initial value. This decrease is related to external factors such as adsorption of water or surface oxidation, and to the tendency to attain an



Table 4  
Work of adhesion

| Sample                          | Symbol                  | $W_A$ (J/m <sup>2</sup> ) |                                   |
|---------------------------------|-------------------------|---------------------------|-----------------------------------|
| PP                              | $W_{A,PP}$              | $0.20 \pm 0.08$           |                                   |
| PP/N <sub>2</sub>               | $W_{A,PP/N_2}$          | $4.84 \pm 0.82$           |                                   |
| 24 h annealed PP/N <sub>2</sub> | $W_{A,PP/N_2/Annealed}$ | $2.97 \pm 0.15$           |                                   |
| 24 h aged PP/N <sub>2</sub>     | $W_{A,PP/N_2/24h}$      | $2.36 \pm 0.67$           |                                   |
| PP/N <sub>2</sub> + pCB         | $W_{A,C-NH_2}$          | $0.41 \pm 0.12$           | Primary amine derivatization      |
| PP/N <sub>2</sub> + tFAA        | $W_{A,C-O}$             | $1.80 \pm 0.95$           | Hydroxyl (+amine) derivatizations |
| PP/N <sub>2</sub> + tFE         | $W_{A,HO-C=O}$          | $2.00 \pm 1.10$           | Carboxyl derivatization           |
| PP/N <sub>2</sub> + dFPH        | $W_{A,C=O}$             | $4.79 \pm 0.64$           | Carbonyl derivatization           |

energetically favorable state by restructuring processes and diffusion [43]. We attribute this decrease to the reorientation of PP/N<sub>2</sub> chains resulting in a lower concentration of chemical functions introduced by the plasma treatment [39,44,45].

### 3.3.2. Role of primary amines in the adhesion mechanism

In Fig. 4a and b, we observe the evolution of both  $W_A$  and the concentrations of Cl and imine groups on the derivatized surfaces as a function of the derivatization time of C–NH<sub>2</sub>. Despite a certain scatter of the experimental data due to the uncertainty of the fitting procedure, clear trends can be deduced. After complete derivatization (24 h),  $W_A$  reaches values close to the ones measured for untreated PP ( $W_{A,PP}$ ). This decrease of  $W_A$  is correlated to the increase of the C<sub>2</sub> and C<sub>4</sub> peaks corresponding to C–Cl and C=N, respectively. These results clearly confirm the important role of C–NH<sub>2</sub> in the adhesion mechanism.

We found that  $W_A$  after 24 h of derivatization ( $0.41 \pm 0.04$  J/m<sup>2</sup>) is still higher than  $W_{A,PP}$  ( $0.2 \pm 0.08$  J/m<sup>2</sup>). This may result from the following: (i) the derivatization reaction with pCB is effective only for the primary amine, while the secondary or tertiary amines can be involved in the adhesion process, (ii) as explained in the introduction, other mechanisms than chemical functionalization can also be responsible for adhesion (roughening [15,16], crosslinking [39], introduction of electric charges on the polymer surface [46]).

### 3.3.3. Role of the other chemical groups in the adhesion mechanism

Table 4 reports  $W_A$  values measured after derivatization of different functional groups compared with PP/N<sub>2</sub> and PP/N<sub>2</sub>/24 h.  $W_A$  decreases with ageing of PP/N<sub>2</sub> from 5.01 J/m<sup>2</sup> to 2.36 J/m<sup>2</sup> after 24 h of exposure to the atmosphere. As we explained in the introduction, this ageing is mainly related to hydrophobic recovery of the surface [42–44]. Since the derivatization reactions occur during 24 h, the reference value should be  $W_{A,PP/N_2/24h} = 2.36$  J/m<sup>2</sup>.

Derivatization of HO–C=O was found to slightly decrease  $W_A$ , but  $W_{A,HO-C=O}$  remains comparable to  $W_{A,PP/N_2/24h}$ . Derivatization of C–OH groups leads to a more significant decrease of  $W_A$ . We attributed the latter effect to partial derivatization of primary and secondary amine functions which occurs simultaneously with the C–OH groups. Therefore, we did not observe a complete loss of adhesion that was expected from the full derivatization of amine groups. Finally, since derivatization of C=O groups (20 min duration) is not observed (see Section 3.3.2), it is not surprising that  $W_{A,C=O}$  ( $4.89$  J/m<sup>2</sup>) remains similar to  $W_{A,PP/N_2}$ .

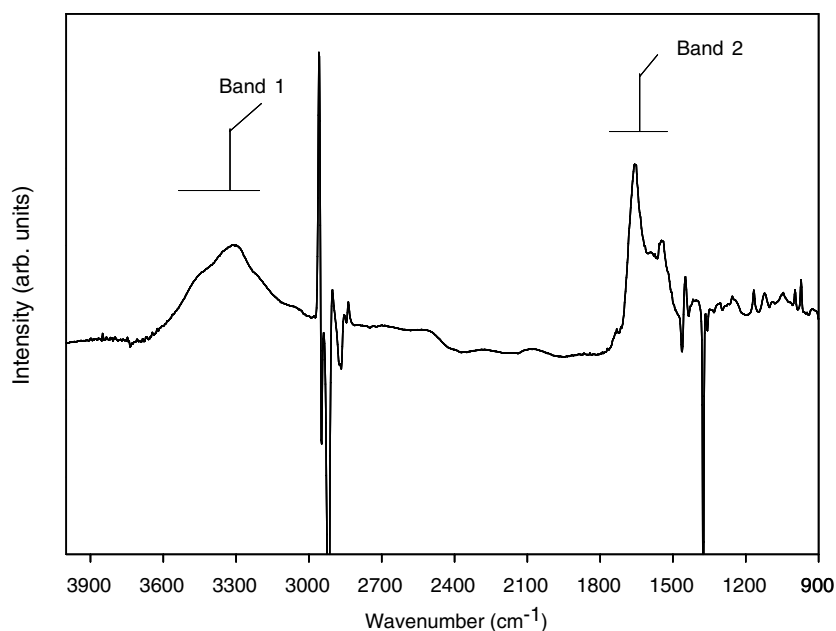


Fig. 5. ATR-IR spectrum obtained as difference between the respective spectra for PP/N<sub>2</sub> and PP/N<sub>2</sub>-Prot.

### 3.3.4. PP/N<sub>2</sub>-protein interaction – ATR study

HG used in this work is formed by PEG and soy protein molecules. Since PEG is only composed of inert aliphatic carbon and ether oxygen (except for their extremities where they contain hydroxyl groups), we assume that the HG component involved in the adhesion process is soy protein. To validate this assumption, we studied the interaction between PP/N<sub>2</sub> and a soy protein solution. Presence of protein on the surface is correlated with the presence of secondary amide forming peptide bonds between amino acids. Since XPS analysis cannot give unambiguous results concerning the type of amide present on a surface, we used ATR-IR.

Since the sampling depth of the ATR-IR technique is relatively large (0.5 μm) compared to the thickness within which protein can react, the signal coming from the modified surface is “diluted” by that of the polymer bulk [47]. To highlight chemical changes of the surface, one must therefore subtract a reference sample spectrum from the treated one. Fig. 5 presents the subtraction of ATR-IR spectra measured for the PP/N<sub>2</sub>-Prot and PP/N<sub>2</sub> samples (used as reference).

As we can see, the protein adsorption on the PP/N<sub>2</sub> surface introduces mainly two new IR bands (1 and 2). Band 1 is rather broad, and it spans between 3620 cm<sup>-1</sup> and 3050 cm<sup>-1</sup>, while being centered at about 3300 cm<sup>-1</sup>. The main component of this band is attributed to the strong –NH stretch of secondary amides observed in polypeptide and proteins (3280–3300 cm<sup>-1</sup>). One can also observe other components contributing to this broad band at about 3250 cm<sup>-1</sup> and 3400 cm<sup>-1</sup>, which can be related to stretching vibrations in primary amine (3280–3460 cm<sup>-1</sup>) and primary amide (3380–3400 cm<sup>-1</sup>) groups, respectively. Band 2 between 1500 cm<sup>-1</sup> and 1750 cm<sup>-1</sup> presents a doublet structure with sub-peaks centered at 1640 cm<sup>-1</sup> and 1550 cm<sup>-1</sup>. We attributed these two peaks to C=O stretching (1630–1680 cm<sup>-1</sup>) and to NH bending (1475–1565 cm<sup>-1</sup>) vibrations in secondary amide, respectively.

From these results, we can unambiguously conclude that proteins are chemically bonded to the PP/N<sub>2</sub> surface, and they participate in the adhesion process.

## 4. Conclusions

We studied the adhesion mechanism between N<sub>2</sub> plasma treated polypropylene (PP/N<sub>2</sub>) and a PEG-soy protein hybrid hydrogel (HG). Using XPS, we have determined the changes in the chemical composition on the PP surface induced by plasma treatment. It has been shown that the main nitrogen-containing functions introduced on the PP surface were amine (C–NH<sub>2</sub>), hydroxyl (C–OH), carboxyl (O–C=O), carbonyl (C=O) and amide (N–C=O) groups. To validate the XPS assignments, we performed chemical derivatization of these chemical functions. We confirmed the presence of primary amine (C–NH<sub>2</sub>) and of the C–OH and O–C=O groups, while the reaction with C=O

was not observed. We concluded that the component at 288.3 eV in the C1s peak is totally attributable to N–C=O.

The chemical derivatization was used to determine the role of the different chemical functions in the adhesion process between PP/N<sub>2</sub> and HG. We showed that the C–NH<sub>2</sub> groups are mainly responsible for the improvement of adhesion. Indeed, the work of adhesion ( $W_A$ ) measured for PP/N<sub>2</sub> after 24 h of ageing ( $2.36 \pm 0.67 \text{ J/m}^2$ ), in comparison with the  $W_A$  measured for C–OH and O–C=O derivatized PP/N<sub>2</sub>, are very close to each other ( $1.80 \pm 0.95 \text{ J/m}^2$  and  $2.04 \pm 1.12 \text{ J/m}^2$ , respectively). After derivatization of C–NH<sub>2</sub>,  $W_A$  falls to  $0.41 \pm 0.12 \text{ J/m}^2$  comparable to untreated PP ( $0.20 \pm 0.08 \text{ J/m}^2$ ).

ATR-IR measurements revealed that the adhesion reactions involved soy proteins present in the HG. Indeed, after interaction with soy solution, we observe appearance of two IR bands related to secondary amides present in protein chains as peptide bonds.

Despite our improved understanding of the adhesion mechanisms, more detailed work should be directed toward the study of (i) the nature of the interaction between HG and PP/N<sub>2</sub> (covalent, ionic, etc.), and (ii) the synergy between chemical functionalization and other modifications induced by N<sub>2</sub> plasma treatment (e.g., nanoroughening, electric charge incorporation, and others).

## Acknowledgements

One of us (R.S.) acknowledges the scholarship from the Belgian National Fund for Scientific Research (FNRS). This work was supported by the Natural Sciences and Engineering Research Council (NSERC) of Canada.

## References

- [1] B.D. Ratner, A.S. Hoffman, *Hydrogels for Medical and Related Applications*, in: J.D. Andrade (Ed.), ACS Symposium series, vol. 31, Washington, DC, 1976.
- [2] G. Fortier, US Patent No. 1996000591941, 1998.
- [3] P. Giusti, N. Barbani, L. Lazzeri, L. Lelli, *J. Macromol. Sci. Pure Appl. Chem.* A31 (Suppl. 6–7) (1994) 839.
- [4] R. Snyders, K. Shingel, O. Zabeida, C. Roberges, M.P. Faure, L. Martinu, J.E. Klemberg-Sapieha, *J. Biomed. Mater. Res. A.*, submitted for publication.
- [5] K.L. Mittal, A. Pizzi, in: *Adhesion Promotion Techniques*, Marcel Dekker Edition, New York, 1999.
- [6] R. D’Agostino, in: *Plasma deposition, treatment and etching of polymers*, Plasma-materials Interaction, Academic Press, San Diego, CA, 1990.
- [7] F. Arefi, M. Tatoulian, V. André, J. Amouroux, G. Lorang, in: K.L. Mittal (Ed.), *Metallized Plastics, Fundamental and Applied Aspects*, vol. 3, Dekker, New York, 1992.
- [8] M.R. Wertheimer, L. Martinu, E.M. Liston, *Plasma sources for polymer surface treatment*, in: *Handbook of Thin Film Process Technology*, IOP Publishing, Ltd., Bristol, 1996.
- [9] M.R. Wertheimer, L. Martinu, J.E. Klemberg-Sapieha, G. Czere-muszkin, *Plasma treatment of polymers to improve adhesion*, in: *Adhesion Promotion Techniques*, Marcel Dekker Edition, New York, 1999.
- [10] E.M. Liston, L. Martinu, M.R. Wertheimer, *J. Adhes. Sci. Technol.* 7 (10) (1993) 1091.

- [11] A.C. Fozza, J.E. Klemberg-Sapieha, M.R. Wertheimer, *Plasmas Polym.* 4 (1999) 183.
- [12] J.E. Klemberg-Sapieha, O.M. Küttel, L. Martinu, M.R. Wertheimer, *J. Vac. Sci. Technol. A* 9 (6) (1991) 2975.
- [13] S. Sapieha, J. Cerny, J.E. Klemberg-Sapieha, L. Martinu, *J. Adhes.* 42 (1993) 91.
- [14] E. Bergeron, J.E. Klemberg-Sapieha, L. Martinu, *J. Vac. Sci. Technol. A* 16 (1998) 3227.
- [15] S.O. Kim, S.W. Na, N.-E. Lee, Y.W. Nam, Y.-O. Kim, *Surf. Coat. Technol.* 200 (7) (2005) 2072.
- [16] S.W. Lee, J.W. Hong, M.Y. Wye, J.H. Kim, H.J. Kang, Y.S. Lee, *Nucl. Instrum. Methods Phys. Res. Sect. B* 219–220 (2004) 963.
- [17] L. Carrino, W. Polini, L. Sorrentino, *J. Mater. Process. Technol.* 153–154 (2004) 519.
- [18] J.E. Klemberg-Sapieha, L. Martinu, N.L.S. Yamasaki, C.W. Lantman, *Thin Solid Films* 476 (2005) 101.
- [19] J. Behnisch, A. Hollander, H. Zimmermann, *Surf. Coat. Technol.* 59 (1–3) (1999) 356.
- [20] N.V. Bath, D.J. Upadhyay, *J. Appl. Polym. Sci.* 86 (2002) 925.
- [21] L.J. Gerenser, *J. Vac. Sci. Technol. A* 6 (1988) 2897.
- [22] M.K. Shi, A. Selmani, L. Martinu, E. Sacher, M.R. Wertheimer, A. Yelon, *J. Adhes. Sci. Technol.* 8 (10) (1994) 1129.
- [23] C. Mühlhan, S. Weidner, J. Freidrich, H. Nowack, *Surf. Coat. Technol.* 116–119 (1999) 783.
- [24] C. Mühlhan, H. Nowack, *Surf. Coat. Technol.* 98 (1998) 1107.
- [25] M.P. Faure, J.F. Brisson, L. Martinu, J.E. Klemberg-Sapieha, O. Zabeida, Patent, WO 02/070590, 2002.
- [26] M. Nitschke, A. Holländer, F. Mehdorn, J. Behnisch, J.J. Meichsner, *J. Appl. Polym. Sci.* 59 (1996) 119.
- [27] P. Chevallier, M. Castonguay, S. Turgeon, N. Dubrulle, D. Mantovani, P.H. McBreen, J.-C. Wittmann, G. Laroche, *J. Phys. Chem.* 105 (2001) 12490.
- [28] S. Pan, D.G. Castner, B.D. Ratner, *Langmuir* 14 (1998) 3545.
- [29] C.D. Batich, *Appl. Surf. Sci.* 32 (1988) 57.
- [30] A. Chilkoti, B.D. Ratner, *Surf. Interface Anal.* 17 (1991) 567.
- [31] T.K. Markkula, J.A. Hunt, F.R. Pu, R.L. Williams, *Surf. Interface Anal.* 34 (2002) 583.
- [32] S.L. Ren, S.R. Yang, Y.P. Zhao, *Appl. Surf. Sci.* 227 (2004) 293.
- [33] R.J. Andereg, *Mass Spectrom. Rev.* 7 (1988) 395.
- [34] E.M. D'Urso, G.J. Fortier, *Bio. Comp. Pol.* 9 (1994) 367.
- [35] K.I. Shingel, M.P. Faure, *Biomacromolecules* 6 (2005) 1635.
- [36] C.D. Wagner, L.E. Davis, M.V. Zeller, J.A. Taylor, R.M. Raymond, L.H. Gale, *Surf. Interface Anal.* 3 (1981) 211.
- [37] D.T. Clark, D. Kilcast, W.K.R. Musgrave, *J. Chem. Soc. Chem. Commun.* (1971) 517.
- [38] R.M. Frances, R.D. Short, *Langmuir* 14 (1998) 4827.
- [39] J. Behnisch, A. Hollander, H. Zimmermann, *Surf. Coat. Technol.* 59 (1–3) (1999) 356.
- [40] P.C. Vollhardt, N.E. Schorre, in: *Organic Chemistry. Structure and Function*, fourth ed., W.H. Freeman and Co., NY and Basingstoke, 2003.
- [41] M. Tatoulian, F. Brétagne, F. Arefi-Khonsari, J. Amouroux, O. Bouloussa, F. Rondelez, A.J. Paul, R. Mitchell, *Plasma Process. Polym.* 2 (2005) 28.
- [42] H.J. Griesser, *Mater. Forum* 14 (1990) 192.
- [43] F. Garbassi, M. Morra, E. Occhiello, in: *Polymer Surface – From Physics to Technology*, Wiley, Chichester, 1994.
- [44] F. Arefi-Khonsari, G. Placinta, J. Amouroux, G. Popa, *Eur. Phys. J. AP4* (2) (1998) 193.
- [45] M.R. Alexander, F.R. Jones, *Carbon* 33 (1995) 569.
- [46] W. Künstler, P. Fröbing, R. Gerhard-Multhaupt, J. Cerny, J.E. Klemberg-Sapieha, L. Martinu, M.R. Wertheimer, A. Holländer, J. Behnisch, in: *Proc. CEIDP, Atlanta, 1998*, p. 609.
- [47] F. Truica-Marasescu, M.R. Wertheimer, *J. Appl. Polym. Sci.* 91 (2004) 3886.